

# Evolution trend analysis of Nearshore seabed in Yangshan Deep-water Port, China

Jun Wang · Jungang Dong · Jing Huang · Zhenlou Chen · Shiyuan Xu

Received: 10 December 2012 / Accepted: 11 October 2013 / Published online: 12 November 2013  
© Springer Science+Business Media Dordrecht 2013

**Abstract** Yangshan Deep-water Port, the largest deep-water port in China, is located in the sea area of the Qiqu Archipelago adjacent to Hangzhou Bay. It goes deep into the ocean and far from the continent, and plays a key role in the economy and shipping of China. The evolution and stability of the seabed in the Yangshan Deep-water Port have potential influences on the security of port engineering. Based on GIS spatial analysis technology and MATLAB numerical analysis software, this study predicted the short-term evolution trend of the Yangshan Port frontier seabed terrain through the establishment of a modified power function model. The research included: (1) a systematic analysis of the characteristics of the terrain evolution before (1960–1997) and after (1998–2008) the construction of Yangshan Port by using terrain data from the study area; (2) based on the historical erosion and deposition characteristics of Yangshan Port, an improved power function model was established and the reliability of the model was validated to simulate the study area's frontier seabed evolution trend in 2015. The results

show that: (1) before the construction of Yangshan Port, the seabed in the study area had a narrower variation in erosion and deposition, with the ratio of erosion and deposition of the stable region, erosion area and deposition area being 53.7 %, 18.3 % and 28.0 % respectively, overall the area showed a relatively stable erosion and deposition character; (2) after the construction of the port, the erosion and deposition variation ranges of the seabed were sharply amplified, obviously due to man-made interference being stronger than natural evolution. The stable region of erosion and deposition was only 22.7 %, erosion area was 53.8 %, and the deposition area was 23.4 %, which showed an erosion intensity that was larger than the deposition intensity; (3) the established improved power function model can be used in the short-term prediction of the Yangshan Port frontier seabed evolution trend with high prediction accuracy. The results can aid in decision making with regard to coastal protection and prospective construction schemes around Yangshan Port.

**Keywords** Seabed evolution · Forecasting · Improved power function model · Yangshan Deep-water Port · China

J. Wang (✉) · J. Dong · J. Huang · Z. Chen · S. Xu  
Key Laboratory of Geographic Information Science of Ministry of Education, East China Normal University, Shanghai 200062, China  
e-mail: wangjunjolly@gmail.com

J. Wang  
e-mail: jwang@geo.ecnu.edu.cn

J. Dong  
e-mail: dongjungang@sina.com

J. Huang  
e-mail: hjing0217@163.com

Z. Chen  
e-mail: zlchen@geo.ecnu.edu.cn

S. Xu  
e-mail: syxu@geo.ecnu.edu.cn

J. Huang  
Department of Geography & Anthropology, Louisiana State University, Baton Rouge, LA 70803, USA

## Introduction

The 21st century is the century of the ocean, and offshore port construction is an effective way to exploit marine resources. To avoid the losses arising from irrational port development, it is necessary to analyze and rigorously predict the variation in submarine topography around the port. However, the variation is controlled by many factors, such as the hydrodynamic function, sediment source, characteristics of submarine topography, human activity and so on. The hydrodynamic function, which can be the foremost one among these factors and includes waves, tides, ocean currents, etc., is also influenced by various other factors, making the hydrodynamic function more complex. The variation in seabed terrain is a

vast, complicated system, so currently the accurate measurement of all factors is impracticable. Nowadays, with the widespread use of geographical information systems (GIS), establishing the digital terrain model using GIS has become an effective method to research the erosion and deposition of the seabed (Xu 2006). Based on the GIS and digital elevation model, the measured terrain data can reflect the sediment transport condition intuitively and accurately.

Dynamic modeling and statistical analysis are two common methods to predict the terrain evolution of the seabed based on GIS. The dynamic modeling method applies to the seabed terrain prediction in a short time scale (several hours to several days) or medium time scale (several weeks to several months) (Nicholson et al. 1997), and the statistical analysis method is suitable for seabed terrain prediction over a long time scale (several years) (Guillas et al. 2011). Many studies on the applicability of dynamic modeling methods in seabed evolution prediction have been done in recent decades, several typical studies are: Nicholson et al. (1997) simulated the evolution of a predicted coast terrain based on 5 different typical models, and compared the simulation results with measured data; Sanford (2008) presented a model that can simulate dynamic changes in the amphibious border sediment base in MATLAB. Statistical analysis methods using the measured data of many years to predict silting and scouring variations in a long-term scale have developed rapidly in recent years, such as that by Wijnberg and Terwindt (1995) who analyzed the abundant terrain data of a large scale range and long time serial based on the sliding form method, and partitioned the coastal area into different terrain evolution characteristics in the Netherlands to study changing trends. More recently, Guillas et al. (2011) presented an Autoregressive Hilbertian (ARH) model to solve the problem of long-term scale silting and scouring variation prediction and then used this model on the East Anglian coast. The method was compared with two existing statistical methods -autoregressive model (Southgate 2008) and the empirical orthogonal function (Reeve et al. 2008), the results showed that the ARH model enables a reduction of 10 % of the root mean squared errors (Guillas et al. 2011). Such research can provide a basis for decision-making in port development.

Yangshan Deep-water Port, which is about 30 km from Shanghai, is the largest deep-water port in China. The seabed evolution and stability of Yangshan Deep-water Port have a potential impact to safety of port engineering. In recent years, many researchers have analyzed the seabed evolution of erosion and deposition in Yangshan Deep-water Port. Yu et al. (2008), Zuo et al. (2009) and Shao et al. (2012) analyzed the seabed erosion and deposition characteristics during the construction period of the Yangshan port and after the completion of the north port. Du et al. (2008) and Zhang et al. (2010) analyzed the influence of the river branch closure works on the seabed erosion and deposition evolution in the

Yangshan port area. These studies have examined the historical erosion and deposition changes and evolution trends in the Yangshan port area, but due to restrictions in the extent and accuracy of the data, the projects are lacking in systematicness, in addition, no scholars have quantitatively forecasted the study area's seabed evolution trend.

The research objective and content of this article include: (1) systematically analyze the terrain evolution characteristics, before and after the construction of the Yangshan Port, using the high precision terrain data in the study area; (2) establish the modified power function model and simulate the study area's seabed evolution trend in 2015, based on the historical erosion and deposition characteristics at the Yangshan Port. The results can provide a reference for decision making for coastal engineering protection and port approach construction schemes around Yangshan Port.

## Study area and dataset

### Study area

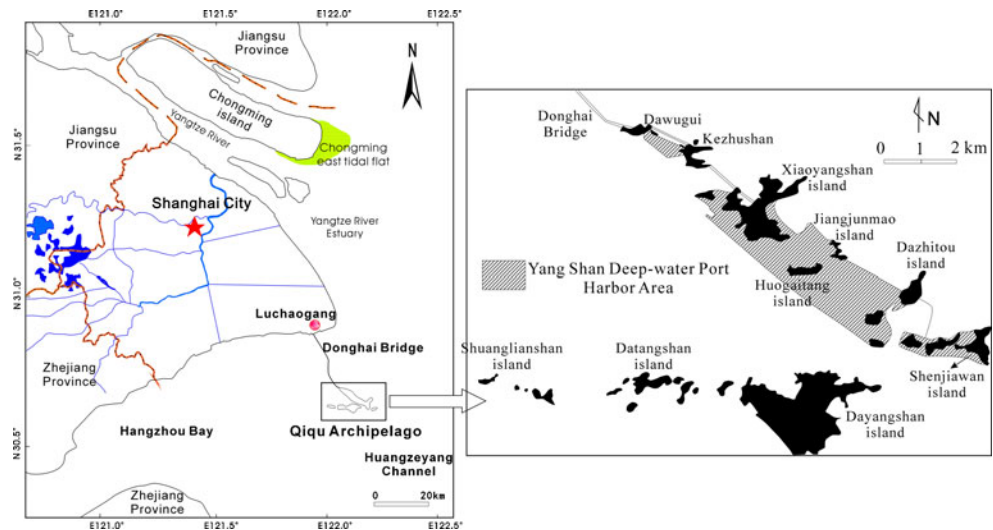
Yangshan Deep-water Port is located in the Qiqu Archipelago, off the estuaries of Hangzhou Bay and the Yangtze River, and is composed of dozens of islands, including Dayangshan Island, Xiaoyangshan Island, etc., and it is the first port built by China on sea islands. Yangshan Deep-water Port lies 32 km southeast of Luchaogang, Pudong, Shanghai 90 km north of the Beilun Port of Ningbo. Eastward it connects directly to the open sea by the Huangzeyang Channel, which is just 45 nautical miles from the international navigation line, and it is the nearest deep-water port to Shanghai. Yangshan Port is seagirt and connected to the mainland by the Donghai Bridge (Fig. 1).

The study area is located in the East Asian monsoon prevailing area along the south rim of the subtropics, its annual mean temperature is 17.2 °C, annual mean precipitation is 985.9 mm, annual mean rainy days are 126.8 days, and annual mean relative humidity is 79 %. The wind direction in this region obviously has a seasonal variation, the ordinary wind direction is NNW-NNE, and the number of days with a wind power in degrees larger than 7° is 65.8 days per year.

The tide in the study area belong to the irregular shallow sea semidiurnal tide at a moderate-intensity level, the annual mean tidal range is 2.75 m, and maximum tidal range is 5.03 m. The major waves are stormy wave, with a height and period on the small side, and the rough sea in this area is mainly caused by typhoon and cold waves. The percentage of no wave days is 30.8 %, and the ordinary wave direction is S, N (36.7 % of wave days).

The area of the Yangshan Deep-water Port was prepared in 1998, and formally started at 2002, and the north port

Fig. 1 Map of the study area



project of the Yangshan Deep-water Port was completely built and put into operation at the end of 2008. The construction projects have accomplished plugging operations in the Xiaoyangshan-Huogaitang, Dawugui-Kezhushan and Jiangjunmao-Dazhitou channels, and have filled the whole Xiaoyangshan-Huogaitang channel to the land of harbor district.

Presently Yangshan Deep-water Port has 16 deep-water container berths, and the overall length of the frontage is 5.6 km, 60 container bridge cranes are provided on the wharf, and the annual handling capacity has reached 9.3 million TEUs. Phase IV of the Yangshan Deep-water Port project will be constructed by 2015, which will allow the annual handling capacity to reach over 13 million TEUs (30 % of Shanghai Ports’ total container handling capacity), and this will make the Yangshan Deep-water Port the fifth largest container port in the world. According to the latest statistics, in 2011 the Yangshan Deep-water Port served 10,166 international ships and 237,512 people.

Primary data sources

The data used in this article can be divided into 2 classes: (1) the seabed measured terrain data in the study area (1960, 1997, 1998, 2005, 2006 and 2008) with the “Beijing 1954 coordinate system”, the base level is the theoretical lowest water level, and vertical data accuracy is 0.01 m; (2) sediment runoff data from the Datong Hydrometric station, Yangtze River (from the Yangtze River Water Conservancy Committee in the Ministry of Water Resources). The measured seabed data is used for historical seabed erosion and deposition evolution characteristics analysis, and seabed erosion and deposition simulation. Sediment runoff data are used for the prediction of the trends of seabed erosion and deposition evolution in Yangshan Port.

Methodology

Analysis method of seabed erosion and deposition evolution

During the analysis of the frontier seabed erosion and deposition evolution characteristics in the study area, the measured terrain data was analyzed with geographic information system software ArcGIS 9.3. The specific methods are given here: (1) import the measured terrain data into ArcGIS, and rectify the depth of water for preprocessing; (2) use the kriging method for interpolation based on the 3D analysis tool in ArcGIS; (3) according to the results of the spatial interpolation, complete the erosion and deposition analysis calculation based on 3D and spatial analysis tools under the unified base level, including the variation in erosion and deposition quantity, erosion and deposition thickness, and erosion and deposition velocity, profile and isobath, and then establish the isobath DEM model, and manufacture and export the calculation results graph. For convenience of analysis, the erosion and deposition region was generally divided into three categories according to the erosion and deposition variation

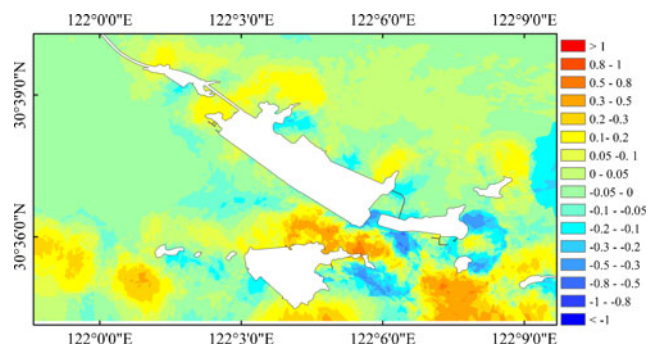


Fig. 2 The spatial distribution of different annual erosion/siltation rates during 1960–1997 (unit: m/year, positive numbers stand for siltation rates, and negative ones erosion rates)

**Table 1** Percentage of erosion areas at different erosion rates

| Classification  | Erosion and deposition rate change (unit: m/year) |          |         |         |         |       |
|-----------------|---|----------|---------|---------|---------|-------|
|                 | 0–0.05  | 0.05–0.1 | 0.1–0.2 | 0.2–0.3 | 0.3–0.5 | >0.5  |
| Erosion area    | 37.8 %  | 8.7 %    | 6.9 %   | 1.7 %   | 1.0 %   | 0.0 % |
| Deposition area | 15.9 %  | 9.6 %    | 10.8 %  | 4.7 %   | 2.8 %   | 0.1 % |

intensity: erosion region (erosion intensity  $>0.05$  m), deposition region (deposition intensity  $>0.05$  m) and relatively stable region (erosion and deposition intensity between  $\pm 0.05$  m).

### Simulation of seabed erosion and deposition trend

The erosion and deposition evolution of the seabed result from the synthetic action of water flow, sediment, seabed gradient and human activities (Kniskern and Kuehl 2003). During the simulation of the seabed erosion and deposition trends, it is impractical to research with comprehensive consideration of the above-mentioned factors. According to a related study, the seabed erosion and deposition trends present an exponential curve, if the seabed in the study area is far away from the equilibrium state when subjected to a strong interference, and the change in rate of depth elevation during this period is regarded as constant, the change in rate will decline in an approximately exponential form with time (Sun and Ren 1997). Based on the above analysis, this article refers to an existing clustering index model (Yuan et al. 2005), and improves on the original methods, and then presents a modified power function model based on the ArcGIS toolbox. This model can be used for analyzing the water depth change in trend for the Yangshan Port area during human intervention from 1998 to 2008, and for predicting the possible trend after the period.

#### (1) Fundamental assumption

The seabed's erosion and deposition condition initially moved away from the equilibrium state after suffering strong human interference, and the interference would last for a period of time, but in a relatively weaker level. The seabed's erosion and deposition condition tends to a homodromous balance after adjustment, which means that the deposition area would not turn into an erosion area in the study period. Erosion and deposition evolution of a seabed possesses regularity over the long-term, and a short-term transformation follows the long-term trend.

#### (2) Method implementation

Supposing  $N$  soundings in the seabed of the study area are recorded as  $P_M$  ( $1 \leq M \leq N$ ); and  $T_m$  and  $t$  respectively represent the number of study years and its serial number, year  $T_0$  in this

article equals  $t=1$ ; the initial rate change of each sounding's elevation at the start of the year  $T_0$  is defined as  $R_0(P_M)$ .

The study area is divided into  $k$  subregions  $A_1, A_2, \dots, A_k$  according to the  $R_0(P_M)$ , and  $R_i$  ( $1 \leq i \leq k-1$ ) represents the classification threshold between  $A_i$  and  $A_{i+1}$ , the selection of the quantity of subranges and the classification threshold should follow the minimum variance principle to the greatest possible extent, this article firstly roughly divided the subranges based on the natural breakpoint method, then adjusted the threshold. After completing the selection of the quantity of subranges and the threshold, the following would be executed:

- 1) Find  $R_i$  in all threshold records, if  $R_i \geq R_0(P_M)$ , i.e. point  $P_M$  falls into region  $A_i$ .
- 2) Otherwise repeat the following procedure while each point  $P_M$  is assigned.
  - a) If  $R_i < R_0(P_M)$ , point  $P_M$  falls into region  $A_{i+1}$ ;
  - b)  $i=i+1$ ;
  - c) Otherwise, go back to Step 1).

Thus  $k$  subregions that can reflect the diversity of the erosion and deposition degree at different spatial positions were obtained, and were represented as  $A_j$  ( $1 \leq j \leq k$ ), then the seabed's average erosion and deposition rate  $R_0(A_j)$  at initial year  $T_0$  in the  $A_j$  region was obtained by the following formula:

$$R_0(A_j) = \frac{1}{n} \sum_{m=1}^n R_0(P_{A_j-m}) \quad (1)$$

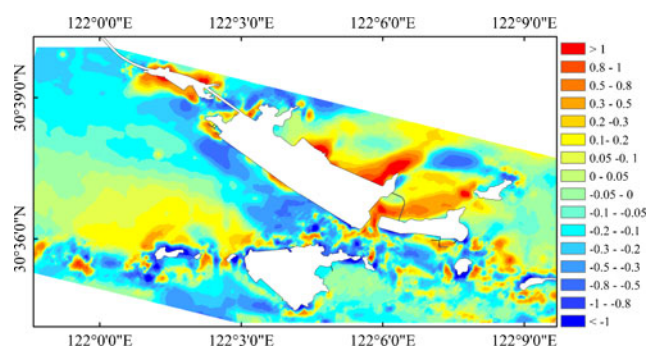


**Fig. 3** Spatial distribution of different annual erosion/siltation rates during 1998–2008 (unit: m/year, positive numbers stand for siltation rates, and negative ones erosion rates)

**Table 2** Percentage of siltation areas at different siltation rates

| Classification  | Erosion and deposition rate change (unit: m/year) |          |         |         |         |       |
|-----------------|---|----------|---------|---------|---------|-------|
|                 | 0–0.05  | 0.05–0.1 | 0.1–0.2 | 0.2–0.3 | 0.3–0.5 | >0.5  |
| Erosion area    | 14.1 %  | 14.6 %   | 17.1 %  | 8.3 %   | 7.0 %   | 6.8 % |
| Deposition area | 8.3 %   | 5.9 %    | 7.1 %   | 2.8 %   | 3.2 %   | 4.4 % |

in which,  $R_0(A_j)$  represents the seabed’s average erosion and deposition rate in the initial year  $T_0$  in the  $A_j$  region (namely the benchmark erosion and deposition rate), a positive rate means deposition, and a negative value means erosion. The  $n$  represents the number of soundings in subregion  $A_j$ ,  $P_{A_j_m}$  represents the  $m^{th}$  sounding in subregion  $A_j$  ( $1 \leq m \leq n$ ),  $R_0(P_{A_j_m})$  means initial erosion and deposition rate of sounding  $P_{A_j_m}$ .

The seabed’s erosion and deposition rate  $R_0(A_j)$  decreases exponentially from the initial rate, the seabed’s average water depth change in rate at year  $T_m$  in a region can be calculated with formula (2), and formula (3) represents the change in water depth between year  $T_0$  to  $T_m$ :

$$R_m(A_j) = R_0(A_j) \times T^a \quad T = T_m - T_0 + 1 \tag{2}$$

$$Z_m(A_j) = Z_0(A_j) + R_0(A_j) \times \sum_{t=2}^T t^a \tag{3}$$

$R_m(A_j)$  represents water depth rate change in year  $T_m$  in region  $A_j$ , and  $Z_m(A_j)$  means the water depth change between years  $T_0$  to  $T_m$  in region  $A_j$ . If the elevation value in a year after  $T_0$  has been given, the different values of parameter  $a$  in each level of the subregion could be ascertained based on formulas (2) and (3), and then the water depth change in rate and change in value for the required years could be calculated from the formulas (2) and (3).

**Results and discussion**

Analysis of historical evolution characteristics in Yangshan Port frontier seabed

The sea area of the Yangshan Deep-water Port is located in the intersection of the Yangtze River estuary and Hangzhou Bay, and has a complex water and sedimentary character. In particular, after the Yangshan Deep-water Port started construction in 2002, the seabed’s evolution suffered a strong interference due to the influence of the hydraulic reclamation project and channel containment. Two periods were determined to analyze the seabed’s erosion and deposition characteristics in this article: the first period is from 1960 to 1997, and the change in erosion and deposition characteristics of the seabed in a natural state before the port construction was

analyzed based on the measured terrain data between 1960 and 1997; the second period is from 1998 to 2008, the change in erosion and deposition characteristics after port construction was analyzed based on the measured terrain data between 1998 and 2008.

(1) Before the port construction (1960–1997)

The measured terrain data from 1960 to 1997 was used to analyze the annual mean erosion and deposition intensities of the underwater topography in the study area (Fig. 2), and to analyze the seabed in a natural state before the construction of the port. The erosion and deposition spatial distribution characteristics from 1960 to 1997 showed that: the eastern half sea area of the island chain narrow channel presented deposition phenomenon (deposition intensity is 0.1 m/year ~0.3 m/year), while the large sea area in the western half and the northeast sea area of the north island chain presented a slight erosion phenomenon (erosion intensity is 0.05 m/year ~0.1 m/year); the erosion and deposition range ability was on the small side, the erosion and deposition stable region covered 53.7 % of the study area, the erosion area 18.3 %, and the deposition area 28.0 %, the overall study area showed a relatively stable erosion and deposition character (Table 1).

(2) After port construction

The measured underwater terrain data of 1998 and 2008 was used to analyze the seabed’s erosion and deposition variation characteristics after the Yangshan Port’s construction (Fig. 3). As can be seen from the color in the illustration, the seabed’s erosion and deposition levels during the construction period were obviously greater than that between 1960 and 1997. The erosion and deposition spatial distribution characteristics from

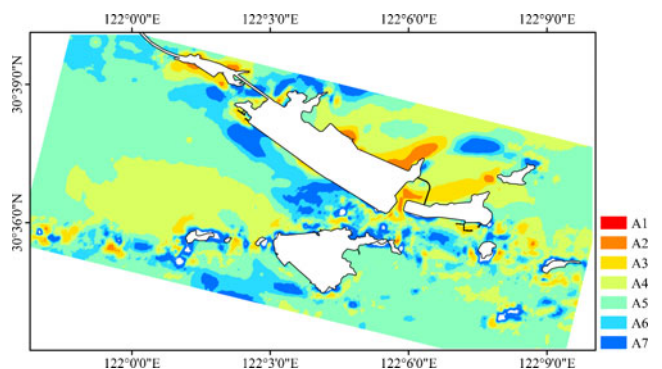
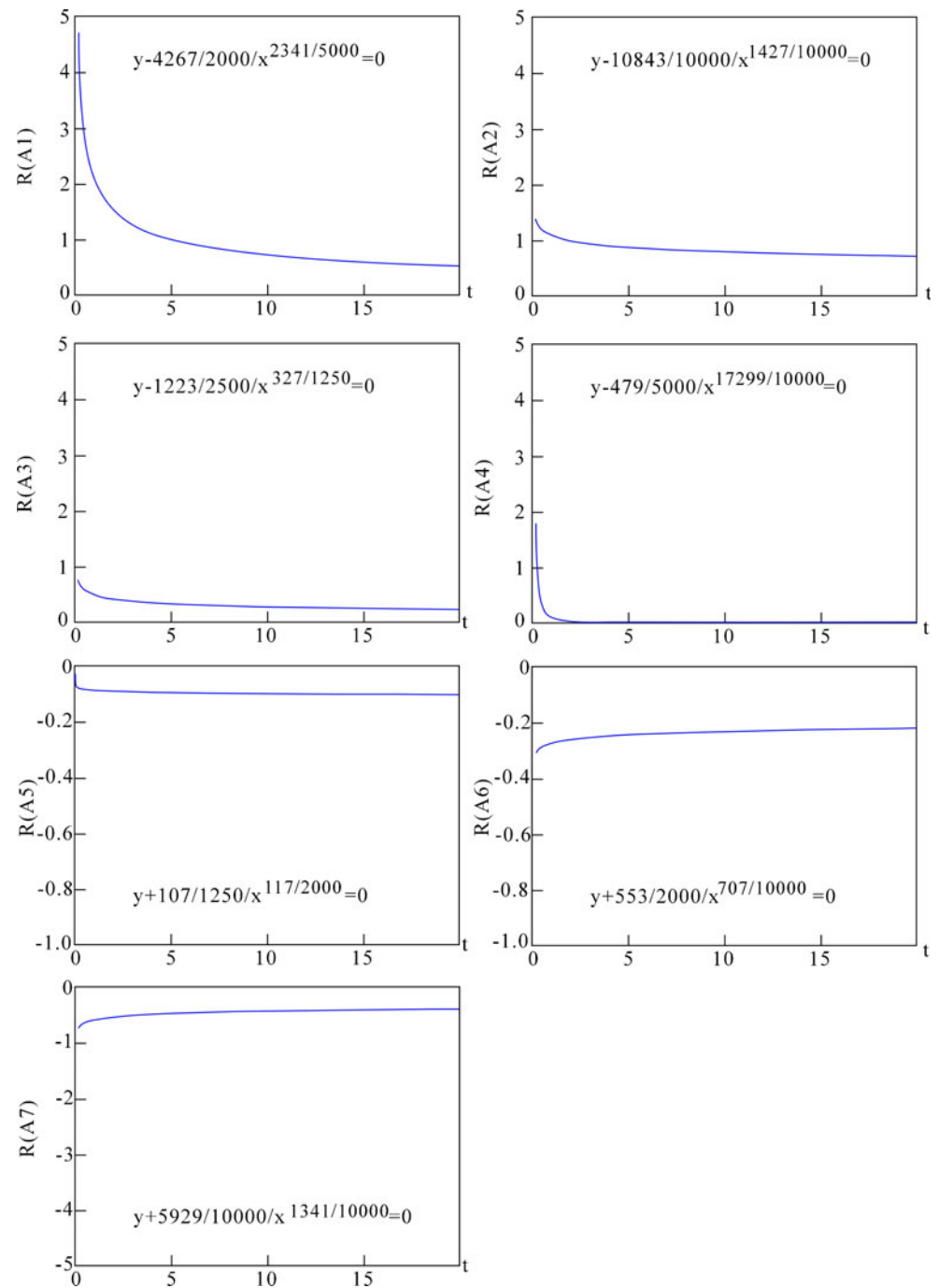


**Fig. 4** Spatial distribution of region  $A_1$ – $A_7$

**Fig. 5** Rate changes of submarine topography in region A<sub>1</sub>–A<sub>7</sub>



1998 to 2008 showed that: the deposition intensity increased notably, landmasses were filled among the islands, and a deposition area appeared with an intensity larger than 0.5 m/year around the hydraulic reclamation project and channel containment area (e.g. Dazhitou Island in the northeast of the island chain and east of Xiaoyangshan Island, ledges of all sizes and Shenjiawan Island's near area); the erosion intensity and range also significantly increased, mainly in the island chain's

narrow channel and the peripheral sea area. So it can be seen that man-made interference has greatly influenced the above-mentioned regions. After port construction, the extent of the seabed's erosion and deposition change increased sharply due to the man-made interference being much stronger than that of natural evolution, and the erosion and deposition stable region covered only 22.7 % of the study area, while the erosion area was 53.8 % and the deposition area was 23.4 %, the erosion

intensity was much larger than the deposition intensity within the study area (Table 2).

Comparing the erosion and deposition ranges under the natural state (before port construction) and during the Yangshan Port project (after port construction), the erosion and deposition range increased after the construction of the port. The specific performance observed can be divided into two aspects: (1) the area of regions with erosion rates larger than 0.05 m/year has noticeably increased; (2) the area of regions with deposition rates larger than 0.3 m/year has also noticeably increased.

The erosion and deposition evolution simulation of the front seabed area in Yangshan Port

After 2008, the erosion and deposition characteristics of Yangshan Port enter a new period of equilibrium due to the suspension of man-made interference. Overall the land boundary will maintain the status quo, and will not change greatly in the subsequent short period of time, and the terrain moves into an erosion and deposition adjustment period. Simultaneously, the Yangshan Port’s sea area presents regional erosion and deposition characteristics, which can also provide the possibility of predicting the erosion and deposition of the seabed in the study area. In order to reflect the influence of human activity on the study area during the period 1998–2008 synthetically, the average rate of change in seabed elevation stations during the period 1998–2008 are treated as the initial rates  $R_0(P_M)$ , and afterwards the change in rates of the elevation points change exponentially according to the initial rates. Due to the fact that human activity and the adjustment of the seabed are occurring simultaneously, the standard exponential curve begins to play a role in the seabed after initially being roughly disturbed, so 1998 is chosen as the initial year,  $T_0$ .

(1) Partition of forecasting subregions

The study area is divided into 7 subregions according to  $R_0(P)$ , the classification thresholds are 1.6 m/year, 0.8 m/year, 0.3 m/year, 0, -0.2 m/year and -0.4 m/year, the positive values express deposition rate changes, and negative values express erosion rate changes (Fig. 4). Regions with deposition rate changes larger than 1.6 m/year are defined as region  $A_1$ , regions with deposition rate changes between 0.8 m/year and 1.6 m/year are defined as region  $A_2$ , and regions with deposition rate changes 0.8~0.3 m/year, 0.3~0.0 m/year, 0.0~-0.2 m/year, -0.2~-0.4 m/year, and <-0.4 m/year are defined as regions  $A_3$ ,  $A_4$ ,  $A_5$ ,  $A_6$ , and  $A_7$  respectively. Then, according to the classification results, every level’s corresponding spatial distribution and standard erosion and deposition rate changes  $R_0(A_i)$  will be obtained.

(2) Calculation of the erosion and deposition rate changes in each subrange

The parameter  $a$  in each subrange has been calculated according to the elevation values measured in 2005, and the figures from  $R_m(A_1)$  to  $R_m(A_7)$  are shown in Fig. 5.

As shown in Fig. 5, the trends of the curves of regions  $A_1$  and  $A_2$  are steep, which means that these regions suffered more from human activity. Consequently regions  $A_1$  and  $A_2$  have higher deposition rates,  $A_1$  is the hydraulic reclamation project region shown in the Fig. 4,  $A_2$  is the region influenced by the hydraulic reclamation project and channel containment;  $A_7$  is the channel deepening region shown in Fig. 4 with a higher erosion rate. It can be seen that these regions suffered directly from human activity.

As shown in Fig. 5, the trends of the curves of regions  $A_3$ ,  $A_4$ ,  $A_6$ , and  $A_7$  are more gentle,  $A_3$  and  $A_4$  are the regions with the lowest deposition rates, which are the areas in the open sea area to the southwest of the island chain’s narrow channel, and to the northwest of the north island chain which suffered slight man-made interference in Fig. 4;  $A_6$  and  $A_7$  are regions with low erosion rates, and represent the island chain’s narrow channel and the narrow channel between the islands. These regions were not directly affected by the project’s construction; however, their erosion and deposition characteristics suffered an indirect influence due to changes in the external environment.

The trend of the curve of region  $A_5$  shows that the region reflects slight erosion characteristics, and its erosion rate does not greatly change. Combined with the distribution in Fig. 4, it shows that basically this region has not been affected by human activity and maintains the relatively balanced erosion and deposition conditions as before the project.

(3) Reliability verification on the model

Due to the fact that the above-mentioned results are based on 1998, 2005 and 2008 terrain data, this article choose the year 2006 to verify the reliability of the model and reduce the impact of the data from these years. The seabed terrain in 2006 is predicted by using the above-mentioned method, and the prediction result is in good agreement with the data measured in 2006, which can be obtained from a comparison of the distribution of the depth contours (Figs. 6 and 7).

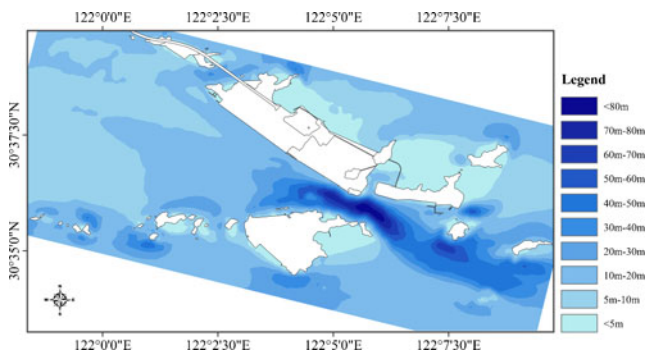
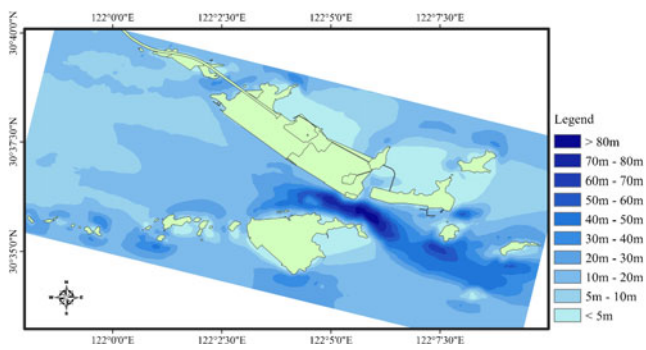


Fig. 6 Measured submarine topography in 2006



**Fig. 7** Predicted submarine topography in 2006

The relative error of each sounding is calculated by formula (4) below, where  $E$  represents the average error of every sounding,  $Z_y$  represents the predicted elevation, and  $Z_s$  represents the measured elevation.

$$E = \left| \frac{Z_y - Z_s}{Z_s} \right| \quad (4)$$

The spatial distribution of relative errors is shown in Fig. 8. An error less than 20 % is acceptable according to the existing standard, and the majority of errors are less than 10 %, regions with larger errors are mostly distributed at the shore or in areas with very serious human disturbance, so overall this model is applicable to the study area.

#### Construction of Yangshan Port digital elevation model in 2015

The border of the study area was temporarily stabilized after the completion of phase III of the construction of Yangshan Port in 2008. Assuming that the border will not change significantly in 2015 compared with 2008, and using the border in 2008 to represent the land border in 2015, this article predicted the study area's seabed terrain in 2015 by using improved power function model with the land border and elevation in 2008 as the initial data. Combined with the land

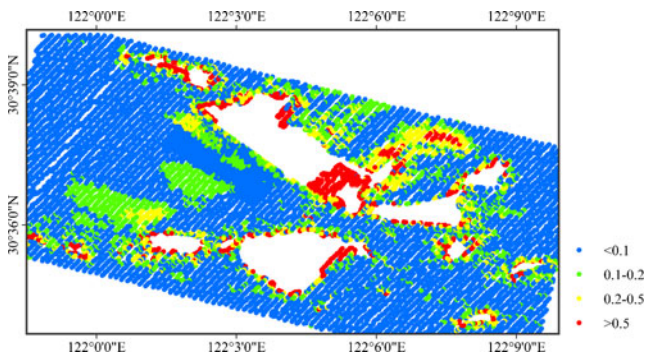


**Fig. 8** Spatial distribution of the relative error

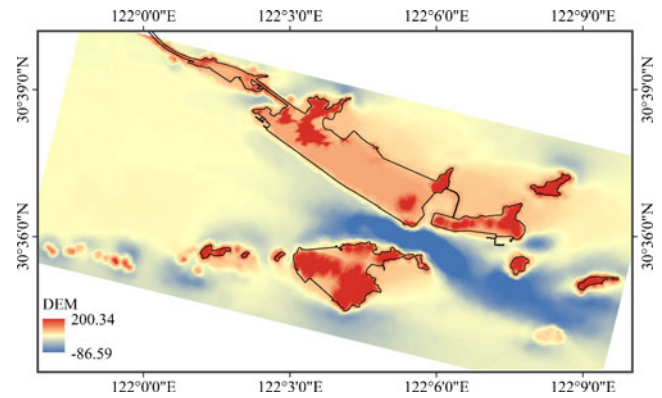


**Fig. 9** Predicted topography of study area in 2015

terrain of the study area, it can construct a digital elevation model of the Yangshan Deep-water Port and its frontier seabed in 2015 (Fig. 9).

#### Conclusion

Before the construction of the Yangshan Deep-water Port, the overall study area showed relatively stable erosion and deposition characteristics, in which the erosion and deposition stable region covered 53.7 % of the study area, the erosion area 18.3 %, and the deposition area 28.0 %. The construction of the Yangshan Deep-water Port disturbed this balance, since the hydraulic reclamation project and channel containment in the early stages of port construction directly altered the intrinsic tidal wave conditions in the sea area, and caused a drastic change in the seabed's erosion and deposition characteristics (Yu et al. 2008), following which the erosion and deposition stable region covered only 22.7 % of the study area, the erosion area covered 53.8 %, and the deposition area 23.4 %.

With the completion of phase III project of the Yangshan Deep-water Port, the hydraulic reclamation project and channel containment never occur again, the seabed will achieve a new relative equilibrium after having experienced an adjustment period of long-term erosion and deposition, since the seabed has strong self-regulation abilities. This provides the possibility for the prediction of the seabed's erosion and deposition characteristics in the study area.

In recent years, seaward sediments from the Yangtze River keep reducing while the runoff changes very little, and the peripheral sea area of around the Yangshan Deep-water Port will maintain a major trend towards erosion for a long period in the future (Chen 2000; Yu et al. 2008; Zuo et al. 2009). The water area in the island chain's narrow channel will continue eroding or maintain erosion and deposition equilibrium with maintenance dredging of the port's channel. As the north island chain's landfill project which centers on the Xiaoyangshan

Island is basically finished, the strong deposition characteristics in the north island chain will reach a new equilibrium with gradual adjustment. A possible impact on the erosion and deposition characteristics of the seabed near Dawugui-Kezhushan Island in the northwest of the study area is expected following phase IV of the west port area's construction. As the reserved shoreline for future development of the Yangshan Deep-water Port, the south island chain which is at the center on the Dayangshan Island will not change noticeably before 2015.

The power function model established by this article has better applicability to the terrain prediction of the Yangshan Deep-water Port seabed in the short term. According to the construction plan of the Yangshan Deep-water Port, the south port area will start construction after 2015. It is likely that strong deposition characteristics will appear around the south island chain as well as the north island chain, and the model will be unable to simulate the seabed terrain after 2015.

**Acknowledgments** We would like to particularly thank Professor Zhiying Yu, State Key Laboratory of Estuarine & Coastal Research, East China Normal University, for his guidance and valuable help. This paper was financially supported by the Innovation Program of Shanghai Municipal Education Commission (Grant No. 13ZZ035), and, the National Natural Science Foundation of China (Grant No. 71373084, 41201550).

## References

- Chen SL (2000) Erosion and accretion characteristics and their causes in the Qiqu Archipelago in the recent century. *Mar Sci Bull* 19(1):58–67
- Du JL, Yang SL, He SL et al (2008) Primary analysis on the erosion-accretion change of the seabed around Yangshan Harbor before and after the plugging offshoot project. *Ocean Eng* 26(4):53–59
- Guillas S, Bakare A, Morley J et al (2011) Functional autoregressive forecasting of long-term seabed evolution. *J Coast Conserv* 15:337–351
- Kniskern T, Kuehl S (2003) Spatial and temporal variability of seabed disturbance in the York River subestuary. *Estuar Coast Shelf Sci* 58:37–55
- Nicholsona J, Brokerb I, Roelvinkc J et al (1997) Intercomparison of coastal area morphodynamic models. *Coast Eng* 31:97–103
- Reeve D, Horrillo-Caraballo J, Magar V (2008) Statistical analysis and forecasts of long-term sandbank evolution at Great Yarmouth, UK. *Estuar Coast Shelf Sci* 79(3):387–399
- Sanford L (2008) Modeling a dynamically varying mixed sediment bed with erosion, deposition, bioturbation, consolidation, and armoring. *Comput Geosci* 34:1263–1283
- Shao RS, Wu MY, Zuo SH (2012) Analysis on seabed deposition and erosion of Yangshan Port during twelve years. *Ocean Eng* 30(1):106–111
- Southgate H (2008) Data-based forecasting of beach volumes on monthly to yearly timescales. *Coast Eng* 55(12):1005–1015
- Sun YM, Ren JW (1997) First exploration of submarine topography evolution model. *Acta Oceanol Sin* 19(1):73–80
- Wijnberg K, Terwindt J (1995) Extracting decadal morphological behavior from high-resolution, long-term bathymetric surveys along the Holland coast using eigenfunction analysis. *Mar Geol* 126:301–330
- Xu BP (2006) Application of GIS and DEM to the analysis of deposition and erosion of foreshore in the Yangtze River estuary. *J Sediment Res* 6:6–10
- Yu H, Chen SL, Gu GC (2008) Water and sediment characteristics and recent erosional and depositional evolution in the Qiqu Archipelago sea area. *Coast Eng* 27(1):10–20
- Yuan HL, Ma JS, Xu WC (2005) Research of cluster index growth model to predict submarine erosion and sediment. *Mar Sci Bull* 24(2):52–56
- Zhang ZL, Zhu QY, Chen JM et al (2010) Influence of blocked bifurcations along Qiqu Archipelago on erosion and sedimentation of sea bed at Yangshan Deep-water Harbor. *J Yangtze River Sci Res Inst* 27(12):5–16
- Zuo SH, Li B, Yang H (2009) Analysis on erosion and accretion characteristics in the channel during construction period of Yangshan Harbor. *J Waterw Harb* 30(1):14–19